

Phase diagram studies for the growth of (Mg,Zr):SrGa₁₂O₁₉ crystals

Detlef Klimm^{a,*}, Bartosz Szczefanowicz^{a,b,1}, Nora Wolff^{a,2},
Matthias Bickermann^a

^aLeibniz-Institut für Kristallzüchtung, Max-Born-Str. 2, 12489 Berlin, Germany.

^bInstitute of Physics, Poznan University of Technology, Piotrowo 3, 60-965 Poznan, Poland

Abstract

By differential thermal analysis a concentration field suitable for the growth of Zr, Mg codoped strontium hexagallate crystals was observed that corresponds well with experimental results from Mateika & Laurien, J. Crystal Growth 52 (1981) 566–572. It was shown that the melting point of doped crystal is ca. 60 K higher than that of undoped crystals. This higher melting points indicates hexagallate phase stabilization by Zr, Mg codoping, and increases the growth window, compared to undoped SrO–Ga₂O₃ melts.

Keywords: hexaferrite structure, thermal analysis, phase diagram, metastability, crystal growth

1. Introduction

Amongst the many pseudobinary compounds in the system SrO–Ga₂O₃, the composition of SrGa₁₂O₁₉ is closest to the component GaO_{1.5} = $\frac{1}{2}$ Ga₂O₃, with a molar fraction of GaO_{1.5} $x = 0.9231$ (Table 1). SrGa₁₂O₁₉ is isostructural to the mineral magnetoplumbite, (Pb,Mn²⁺,Mg)(Fe³⁺,Mn³⁺)₁₂O₁₉, space group $P6_3/mmc$, which again belongs to the larger group of hexagonal ferrites, or “hexaferrites” [1]. Many of these materials possess strong and highly anisotropic persistent magnetic and electric moments, which makes them interesting as permanent magnets or even multiferroics. Crystal growth of Fe³⁺ based hexaferrites is a challenge, because at the high melting points beyond 1500 °C of these materials partial reduction to Fe²⁺ occurs; typically liquidus temperatures are reduced by foreign solvents like Na₂O to stabilize iron valency [2]. Resulting from the structural similarity, SrGa₁₂O₁₉ is a good substrate crystal for the epitaxial deposition of other hexaferrites [3]. Moreover, the chemical versatility of the magnetoplumbite structure allows doping of SrGa₁₂O₁₉ with luminescent ions such as Mn²⁺ and Cr³⁺ [4, 5].

The first publication of a phase diagram for the system SrO–Ga₂O₃ [6] showed that SrGa₂O₄ is the only intermediate compound with a congruent melting point. In more recent studies this system was redetermined and partially thermodynamically assessed [7, 8], with mainly sim-

ilar results like the previous study [6] – but with the difference that the peritectic melting of SrGa₁₂O₁₉ was reported there at significantly lower temperature (Table 1). However, all studies agree with the observation that it melts peritectically under the formation of β -Ga₂O₃. A somewhat lower peritectic melting temperature $T_f^p = 1540$ °C for SrGa₁₂O₁₉ and $T_f^p = 1530$ °C for BaGa₁₂O₁₉ was reported elsewhere; both compounds form an isomorph solid solution series [9, 10]. For the SrO–Ga₂O₃ system, minor differences are reported mainly on the SrO side, the reader is referred to the PhD theses of Solak [11] and Richter [12].

As a result of peritectic melting, crystal growth of SrGa₁₂O₁₉ is only possible from melts with an excess of SrO, compared to the stoichiometry of the compound. According to the assessment of Zinkevich [8], this phase with a Ga₂O₃ molar fraction $x = 0.9231$ is in equilibrium with the melt only between the peritectic points of SrGa₁₂O₁₉ ($x_f^p = 0.8002$, $T_f^p = 1553$ °C) and the neighboring phase SrGa₄O₇ ($x_f^{p'} = 0.7723$, $T_f^{p'} = 1492$ °C). (The concentration data from [8] that are based on the components SrO and Ga₂O₃ were converted to SrO and GaO_{1.5} which are used here.) With the lever rule, from these data a maximum yield $Y = (0.8002 - 0.7723)/(0.9231 - 0.7723) \approx 18\%$ for the growth of SrGa₁₂O₁₉ crystals from melts with excess SrO can be calculated.

First SrGa₁₂O₁₉ crystals with size up to 3 mm were grown by Haberey et al. [13] from fluxes with $x = 0.830$, which means a slightly higher GaO_{1.5} concentration than the peritectic point given by Zinkevich [8], $x_f^p = 0.8002$. This difference indicates that supercooling of the melt might avoid the primary crystallization of β -Ga₂O₃. Later the same authors performed growth experiments with the addition of alkali molybdates or bismuth oxide. From melt solutions with Bi₂O₃ as component, SrGa₁₂O₁₉ crystals up to 15 mm diameter (useful area up to 30 mm²) could be ob-

*Corresponding author

Email address: detlef.klimm@ikz-berlin.de (Detlef Klimm)

¹Present address: INM – Leibniz Institute for New Materials, Campus D2 2, 66123 Saarbrücken, Germany

²Present address: Helmholtz-Zentrum für Materialien und Energie, Hahn-Meitner-Platz 1, 14109 Berlin, Germany

tained. However, these crystals incorporated ca. 0.5 mol% Bi [14].

Significantly better and larger crystals were obtained by Mateika and Laurien [15]. They stated that the small concentration region in the pseudobinary system where $\text{SrGa}_{12}\text{O}_{19}$ crystallizes first (in their paper $0.7730 \leq x_{\text{GaO}_{1.5}} \leq 0.8095$, very similar to the data given above) can be increased, if Ga^{3+} is substituted partially by small equimolar additions of Mg^{2+} and Zr^{4+} . The partitioning coefficients of both ions was found to be $k \approx 1.05 > 1$, which suggests that the hexaferrite structure is stabilized. The possibility to substitute Ga^{3+} by equimolar amounts of Mg^{2+} and Zr^{4+} was already earlier demonstrated for $\text{Gd}_3\text{Ga}_5\text{O}_{12}$ [16].

2. Experimental

Differential thermal analysis (DTA) with simultaneous thermogravimetry (TG) was performed using NETZSCH STA 449C “Jupiter” and STA 409CD thermal analyzers. DTA/TG sample holders with Pt/Pt90Rh10 thermocouples and lidded platinum crucibles allowed measurements up to 1650 °C in a flowing mixture of 20 ml/min Ar + 20 ml/min O₂. (Ga_2O_3 evaporates mainly under dissociation as Ga_2O , and SrO mainly as metallic Sr; and both reactions can be suppressed by adding O₂ to the atmosphere.) Usually the DTA samples were molten twice to ensure good mixing, and the second heating curves were used for further analysis. Unfortunately, under these experimental conditions the liquidus temperatures of mixtures close to the high melting components SrO and Ga_2O_3 (cf. Table 1) cannot be accessed, which prohibits good mixing and equilibration of DTA samples. Alternative DTA setups with higher maximum temperature cannot be used, because sample holder and/or furnaces contain then parts that are sensitive with respect to oxygen (e.g. from tungsten or graphite). Under such conditions, however, both components are prone to decomposition to metallic Sr or Ga, or Ga_2O suboxide, respectively, and subsequent evaporation. Ca. 50 different compositions spanning the whole range from pure SrO to pure Ga_2O_3 were prepared by melting together appropriate quantities of SrCO_3 and Ga_2O_3 powders (Alfa, 99.99% purity) in the DTA crucibles.

In a second series MgO, ZrO₂, and an equimolar mixture of MgO + ZrO₂ was added to a $(1-x)\text{SrO} + x\text{GaO}_{1.5}$ mixture with $x = 0.857$, that is close to the growth window of $\text{SrGa}_{12}\text{O}_{19}$. It was the aim of this series to reveal the influence of these dopants on the growth window.

3. Results and discussion

As mentioned in the previous section, the liquidus temperatures close to pure strontium or gallium oxide, respectively, are so high that evaporation from the sample prevents reliable thermal analysis. Not so in the center of

the system where a low eutectic (1326 °C, $x = 0.49$) between $\text{Sr}_{10}\text{Ga}_6\text{O}_{19}$ and $\text{Sr}_3\text{Ga}_4\text{O}_9$ results in low liquidus temperatures without significant evaporation (cf. Fig. 2). Nevertheless, another peculiarity made interpretation of DTA signals not straightforward there: It turned out that DTA curves were often not well reproducible, especially for compositions from the central region of the phase diagram. This is demonstrated for $(1-x)\text{SrO} + x\text{GaO}_{1.5}$ mixtures with $x = 0.5549$ (two subsequent heatings of one sample) and $x = 0.5855$ (three heatings) in Fig. 1.

It is obvious that the curve (1) for sample $x = 0.5549$, and curves (2) and (3) for sample $x = 0.5855$, show exothermal peaks during these heating runs, which is untypical. All melting processes are endothermic events, but exothermal effects may occur if a sample is not in thermodynamic equilibrium and returns to equilibrium during heating.

For the $x = 0.5549$ sample the peaks with onsets at 1241 °C and 1326 °C appear for both heating runs, because there equilibrium is obviously obtained, also for the upper curve. Not so the peak with onset at 1182 °C which results from a non-equilibrium situation where SrGa_2O_4 and $\text{Sr}_{10}\text{Ga}_6\text{O}_{19}$ are coexisting. From Fig. 2 it can be seen that this is possible only if $\text{Sr}_3\text{Ga}_4\text{O}_9$ as well as $\text{Sr}_3\text{Ga}_2\text{O}_6$ are not formed. This can occur as a result of strong supercooling of both phases, which results in the non-equilibrium crystallization of their neighbors. Then, however, it is normal that these neighbor phases form together a lower eutectic (indicated by the dashed isotherm at 1182 °C and the non-equilibrium prolongations of the liquidus lines in Fig. 2), than the equilibrium phases $\text{Sr}_3\text{Ga}_4\text{O}_9$ and $\text{Sr}_3\text{Ga}_2\text{O}_6$ would do.

Curve (1) for the $x = 0.5855$ sample shows the same non-equilibrium eutectic, but immediately at the high temperature side of this peak a small exothermal bend occurs. No other effects appear until 1416 °C, which is the peritectic melting temperature of $\text{Sr}_3\text{Ga}_4\text{O}_9$. This melting temperature was found here higher than reported in recent studies[6, 12], but we assume that these authors mixed up the eutectic at 1326 °C with the peritectic melting of $\text{Sr}_3\text{Ga}_4\text{O}_9$. It should be noted that the composition of this sample is just 1.4% right from $\text{Sr}_3\text{Ga}_4\text{O}_9$, and hence this phase should be predominating there under equilibrium conditions. Only in curve (2) of this sample, $\text{Sr}_3\text{Ga}_2\text{O}_6$ is formed as a non-equilibrium phase first, which decomposes soon at 1241 °C to $\text{Sr}_3\text{Ga}_4\text{O}_9$ and $\text{Sr}_{10}\text{Ga}_6\text{O}_{19}$, which then melt eutectically at 1326 °C. The last heating curve (3) for this sample is similar to the previous one – with the difference that the exothermal jump into equilibrium occurs slightly later, and consequently the decomposition peak of $\text{Sr}_3\text{Ga}_2\text{O}_6$ cannot be observed.

After passing all DTA peaks, the $x = 0.5855$ curves show an upward bend near 1490 °C. This indicates the liquidus temperature at this composition, because all melting processes are completed and the DTA curves return to their basis line. For the $x = 0.5549$ sample an analogous (but weaker) bend occurs near 1400 °C because this composition is closer to the eutectic point.

Table 1: Compounds in the pseudobinary system $(1-x)\text{SrO}-x\text{Ga}_2\text{O}_3$. T_f^c , T_f^p , or T_f^i marks congruent melting points, or peritectic or peritectoid decomposition temperatures. T_t are transition temperatures between different phases of one compound. For structural data of these compounds see e.g. Ropp[17].

| Formula | x | remarks and reference |
|--|--------|---|
| SrO | 0.0000 | $T_f^c = 2665^\circ\text{C}$ [18] |
| $\text{Sr}_4\text{Ga}_2\text{O}_7$ | 0.3333 | $T_f^p = 1540^\circ\text{C}$ [7], or 1476°C [6] |
| $\text{Sr}_7\text{Ga}_4\text{O}_{13}$ | 0.3636 | $T_f^p = 1490^\circ\text{C}$ [7], not found here |
| $\text{Sr}_{10}\text{Ga}_6\text{O}_{19}$ | 0.3750 | structure reported from [19, 20] |
| $\text{Sr}_3\text{Ga}_2\text{O}_6$ | 0.4000 | $T_f^i = 1230^\circ\text{C}$ [7] |
| $\text{Sr}_3\text{Ga}_4\text{O}_9$ | 0.5714 | $T_f^p = 1350^\circ\text{C}$ [7], or 1322°C [6] |
| SrGa_2O_4 | 0.6667 | $T_t = 1430^\circ\text{C}$, $T_f^c = 1550^\circ\text{C}$ [7], 1580°C [6] |
| SrGa_4O_7 | 0.8000 | $T_f^p = 1490^\circ\text{C}$ [7], or 1442°C [6] |
| $\text{SrGa}_{12}\text{O}_{19}$ | 0.9231 | $T_f^p = 1550^\circ\text{C}$ [7], 1553°C [8], or 1462°C [6] |
| Ga_2O_3 | 1.0000 | $T_f^c = 1800^\circ\text{C}$ [18] |

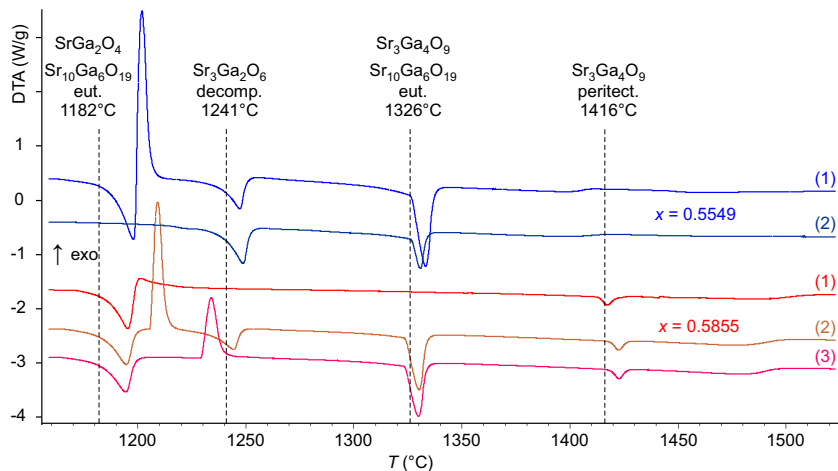


Figure 1: Subsequent DTA heating curves for identical samples with $x = 0.5549$ (top two curves) or $x = 0.5855$ (bottom three curves), respectively. Occasional exothermal peaks result from non-equilibrium that was obtained during previous cooling.

A tentative phase diagram of the system $\frac{1}{2}\text{Ga}_2\text{O}_3$ –SrO is shown in Fig. 2 which is partially based on the references[6, 7, 10, 11, 12], but complemented and corrected with experimental DTA points from this study. It is obvious that not all experimental points can be explained by the liquidus and isothermal lines in the diagram. However, additional non-equilibrium events can be expected to occur, e.g., if only one of the equilibrium eutectic phases at 1326°C is absent. Other effects, like the peaks on the 1410°C level right from $x = 0.8$, result from the initial crystallization of the hexagallate $\text{SrGa}_{12}\text{O}_{19}$. The remaining melt is depleted by Ga_2O_3 and its composition moves along the liquidus towards the eutectic point near $x = 0.76$, which produces then the corresponding peak also for compositions right from SrGa_4O_7 .

In agreement with the Mateika & Laurien paper [15], Fig. 2 shows that the $\text{SrGa}_{12}\text{O}_{19}$ liquidus, and hence its crystallization window, is extremely narrow. Moreover, crystal growth is hampered there by the non-equilibrium crystallization of the neighbor phase SrGa_4O_7 [15]. As pointed out before, the occasional crystallization of non-equilibrium phases seems to be a general issue of the Ga_2O_3 –

SrO system.

In the magnetoplumbite crystal structure, the Ga^{3+} ions reside in octahedral, bipyramidal, and tetragonal environments, and the five-fold coordinated Ga^{3+} is randomly displaced from the center of its trigonal bipyramidal coordination polyhedron along positive and negative directions of the c -axis [1, 21, 22]. Mateika & Laurien [15] succeeded to increase the growth window of $\text{SrGa}_{12}\text{O}_{19}$ by partial substitution of Ga^{3+} (ionic radius $r^{[6]} = 76$; $r^{[4]} = 61$ pm [23]) by simultaneous substitution with identical amounts of Mg^{2+} ($r^{[6]} = 86$; $r^{[4]} = 71$ pm) and Zr^{4+} ions ($r^{[6]} = 86$; $r^{[4]} = 73$ pm), and crystals $> 1\text{ cm}^3$ could be grown from a $\text{Sr}_{1.56}\text{Ga}_{10.40}\text{Mg}_{0.52}\text{Zr}_{0.52}\text{O}_{18.72}$ melt [15].

It was the purpose of further DTA measurements in this study to investigate how Mg^{2+} and/or Zr^{4+} doping influences relevant phase equilibria in the $\frac{1}{2}\text{Ga}_2\text{O}_3$ –SrO system. From Fig. 2 it is evident that crystal growth of $\text{SrGa}_{12}\text{O}_{19}$ should be possible along its liquidus between the peritectic lines at 1469°C and 1434°C , which is a very narrow growth window. In three series of DTA measurements, to a SrO/ Ga_2O_3 mixture with $x = 0.8571$ (where both peritectic peaks are strong) growing amounts of MgO

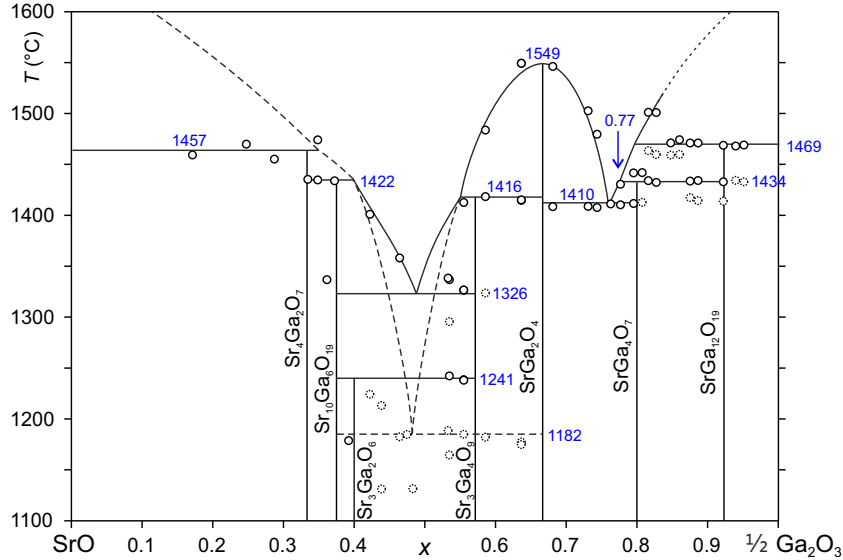


Figure 2: Experimental phase diagram $\text{Ga}_2\text{O}_3\text{-SrO}$ with 7 intermediate compounds. Dashed liquidus lines indicate strong evaporation resulting from high temperatures close to the end members, or metastability near $x = 0.5$, respectively. Besides, one metastable eutectic at 1182°C is drawn.

only, ZrO_2 only, and of an equimolar MgO/ZrO_2 mixture were added.

Doping by exclusively MgO or ZrO_2 was not useful: In both cases the 1434°C peak (SrGa_4O_7 peritectic) is lowered by $\approx 10\text{K}$, but the 1469°C peak ($\text{SrGa}_{12}\text{O}_{19}$ peritectic) disappeared for additive levels around 4% – indicating instability of the hexagallate phase. Not so for equimolar MgO/ZrO_2 doping, which is shown in Fig. 3. It turns out that again the lower peritectic moves downwards, here by $\approx 20\text{K}$. Even more impressive is that the higher peritectic, which is the upper stability range of the hexagallate phase, shifts $\gtrsim 60\text{K}$ upwards. As already pointed out by Mateika & Laurien [15], obviously the co-doping with $\text{Mg}^{2+}/\text{Zr}^{4+}$ increases the stability range. One can see from Fig. 3 that an upper useful co-doping level, is of the order $y = 0.1$, which means each 10% of MgO and ZrO_2 can be added. One can assume that the highly versatile coordinations [6], [5], [4] of Ga^{3+} in the hexaferrite structure support the partial replacement of this ion by the $\text{Mg}^{2+}/\text{Zr}^{4+}$ dopant. Besides, the high number of four components leads at liquidus temperatures around 1500°C to a significant entropic stabilization of the $(\text{Mg,Zr})\text{:SrGa}_{12}\text{O}_{19}$ mixture phase.

The graphical representation of this codoping is not straightforward, because quaternary systems cannot be drawn without constraints in two dimensions. Mateika & Laurien [15] used a simplified concentration triangle with $(\text{MgO}\cdot\text{ZrO}_2)\text{-Ga}_2\text{O}_3\text{-SrO}$ as pseudocomponents or components, respectively. This is reasonable, because MgO and ZrO_2 are used only in the 1:1 molar ratio, and it is justified, because only the rim systems $\text{SrO-Ga}_2\text{O}_3$, SrO-ZrO_2 , and $\text{MgO-Ga}_2\text{O}_3$ are relevant for the discussion. Fig. 4 a) is a similar presentation of this concentration triangle, with the difference that $\frac{1}{2}\text{Ga}_2\text{O}_3$ and $\frac{1}{2}(\text{MgO}\cdot\text{ZrO}_2)$ are defined as components. This has the benefit that all

corners represent one single cation.

The further discussion may neglect the potential rim system MgO-SrO because this is simple eutectic without intermediate compounds, and hence no other phases that could crystallize first [24]. The other potential rim system $\text{ZrO}_2\text{-Ga}_2\text{O}_3$ is not known from the literature. However, simple Ga-Zr oxides do not exist and Ga-O-Zr bonds can be stabilized only with organic ligands [25]. Hence, one can assume that also the $\text{ZrO}_2\text{-Ga}_2\text{O}_3$ system is eutectic, like $\text{ZrO}_2\text{-Al}_2\text{O}_3$ [26]. Indeed, from Ga_2O_3 rich ternary melts with high MgO/ZrO_2 doping only MgGa_2O_4 crystallized in addition to $\text{SrGa}_{12}\text{O}_{19}$ and $\beta\text{-Ga}_2\text{O}_3$, and no Ga-Zr oxide phase was found [15]. Consequently, also the potential rim system $\text{ZrO}_2\text{-Ga}_2\text{O}_3$ can be neglected.

Both remaining rim systems that include $\text{MgO}\cdot\text{ZrO}_2$ contain one intermediate compound with congruent melting behavior: SrZrO_3 ($T_f = 2671^\circ\text{C}$, [27]) and MgGa_2O_4 ($T_f \approx 1930 \dots 1950^\circ\text{C}$, [28, 29]). If intermediate compounds in ternary systems can coexist in equilibrium, tie lines can be drawn between them and the concentration triangle can be divided to partial systems. It is very common that such tie lines can be drawn between congruently melting phases, although exceptions are possible e.g. near ternary peritectic points [30]. In such cases, however, three solid phases should coexist, which was not reported in the literature [15, 31] so far.

Fig. 4 a) shows the concentration triangle with these tie lines that separate independent partial systems. The considerations given above allow to conclude that for melts inside the shaded area, the whole crystallization path remains within this triangle, because this is a partial system. The triangle is enlarged in Fig. 4 b). The experiments by Mateika & Laurien resulted in the red corner as upper useful limits for the Ga_2O_3 and dopant concentrations (in ref-

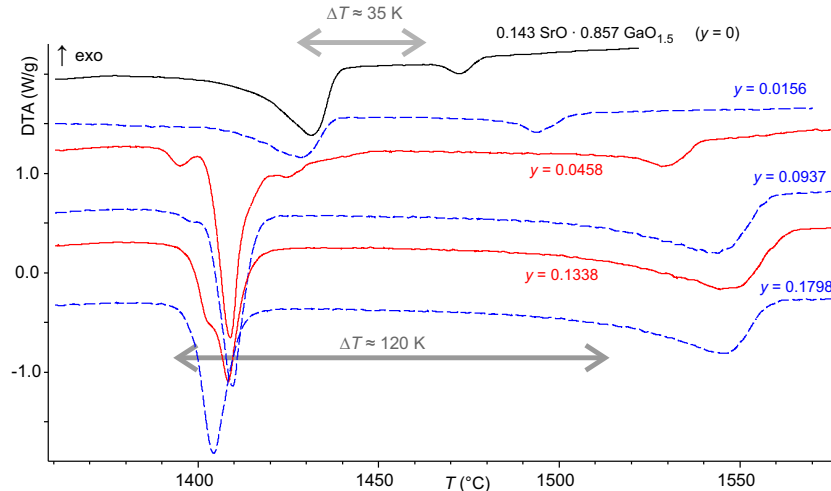


Figure 3: Starting from a $(1 - x)\text{SrO} + x\text{GaO}_{1.5}$ mixture with $x = 0.857$ (cf. Fig. 2), growing molar concentrations y of a $\text{MgO}:\text{ZrO}_2=1:1$ mixture were added. This increases the difference between the lower SrGa_4O_7 and the higher $\text{SrGa}_{12}\text{O}_{19}$ peritectic decomposition significantly.

erence [15] Fig. 1 a). In this publication the chemical composition of melts was compared with the composition of $(\text{Mg},\text{Zr}):\text{SrGa}_{12}\text{O}_{19}$ crystals that were grown, and enrichment of the dopants in the crystal was found. Besides, the peritectic melting behavior of $\text{SrGa}_{12}\text{O}_{19}$ requires melts with a smaller Ga_2O_3 concentration than the crystal. As a consequence, an upward right shift of the crystal compositions compared to the melts was observed [15].

Unfortunately, there is a contradiction: Fig 1 in [15] shows that $(\text{Mg},\text{Zr}):\text{SrGa}_{12}\text{O}_{19}$ crystallizes only from melts inside the “red corner” in Fig. 4 of this article; but the melt composition $\text{Sr}_{1.56}\text{Ga}_{10.40}\text{Mg}_{0.52}\text{Zr}_{0.52}\text{O}_{18.72}$ that is given in Tab. 2 of the Mateika & Laurien paper corresponds to the left red square in Fig. 4, and the resulting crystal to the right square. We assume that concentration data were mixed up and can only guess that dopant concentration have to be doubled. Then the melt concentration lies almost exactly in the corner, and the result is (within the typical experimental error) almost exactly on the blue rim of the partial triangle. One can conclude that by trial and error Mateika & Laurien found a melt composition that is almost optimum for crystal growth in this system.

The DTA measurements that are shown in Fig. 3 are a confirmation: The growth window for $(\text{Mg},\text{Zr}):\text{SrGa}_{12}\text{O}_{19}$ could be increased mainly by an increased stability of this hexagallate phase. This works well up to the $y = 0.0937$ doping level. The starting composition of this doping series, $x = 0.857$, and the useful upper doping level are marked by green circles in Fig. 4. Higher doping along the green dashed line is detrimental because the partial system is left.

4. Conclusions

Mateika & Laurien [15] identified a concentration field in the quaternary system $\text{SrO}-\text{Ga}_2\text{O}_3-\text{MgO}-\text{ZrO}_2$ were

the growth of bulk $(\text{Mg},\text{Zr}):\text{SrGa}_{12}\text{O}_{19}$ crystals is possible. With DTA measurements this concentration field was confirmed to be optimum, and a further optimization with respect to starting composition seems not possible. One technical error concerning concentration data in Tab. 2 of [15] was identified.

Acknowledgments

The authors thank Christo Gugushev for helpful discussions on this topic, and Steffen Ganschow for hints improving the manuscript. B.S. acknowledges support from the EU in the framework of the Erasmus+ program.

References

- [1] C. Delacotte, G. F. S. Whitehead, M. J. Pitcher, C. M. Robertson, P. M. Sharp, M. S. Dyer, J. Alaria, J. B. Claridge, G. R. Darling, D. R. Allan, G. Winter, M. J. Rosseinsky, Structure determination and crystal chemistry of large repeat mixed-layer hexaferrites, *IUCrJ* 5 (2018) 681–698. doi:10.1107/S2052252518011351.
- [2] R. Gambino, F. Leonhard, Growth of barium ferrite single crystals, *J. Amer. Ceram. Soc.* 44 (5) (1961) 221–224. doi:10.1111/j.1151-2916.1961.tb15364.x.
- [3] A. S. Kamzin, L. V. Lutsev, V. A. Petrov, Epitaxial films of Ba-M type hexagonal ferrites, *Physics of the Solid State* 43 (12) (2001) 2253–2256. doi:10.1134/1.1427952.
- [4] J. M. P. J. Verstegen, Luminescence of Mn^{2+} in $\text{SrGa}_{12}\text{O}_{19}$, $\text{LaMgGa}_{11}\text{O}_{19}$, and $\text{BaGa}_{12}\text{O}_{19}$, *J. Solid State Chem.* 7 (1973) 468–473. doi:10.1016/0022-4596(73)90176-X.
- [5] J. Xu, D. Chen, Y. Yu, W. Zhu, J. Zhou, Y. Wang, $\text{Cr}^{3+}:\text{SrGa}_{12}\text{O}_{19}$: A broadband near-infrared long-persistent phosphor, *Chemistry – An Asian Journal* 9 (2014) 1020–1025. doi:10.1002/asia.201400009.
- [6] P. Batti, G. Slocari, Diagramma di stato del sistema $\text{SrO}-\text{Ga}_2\text{O}_3$, *Annali di Chimica* 59 (1969) 155–162.
- [7] V. P. Kobzareva, L. M. Kovba, L. M. Lopato, L. N. Lykova, A. V. Shevchenko, Phase diagram of the system $\text{SrO}-\text{Ga}_2\text{O}_3$, *Zh. Neorg. Chim.* 21 (1976) 1651–1654.
- [8] M. Zinkevich, Calorimetric study and thermodynamic assessment of the $\text{SrO}-\text{Ga}_2\text{O}_3$ system, *Internat. J. Mat. Res.* 98 (2007) 574–579. doi:10.3139/146.101513.

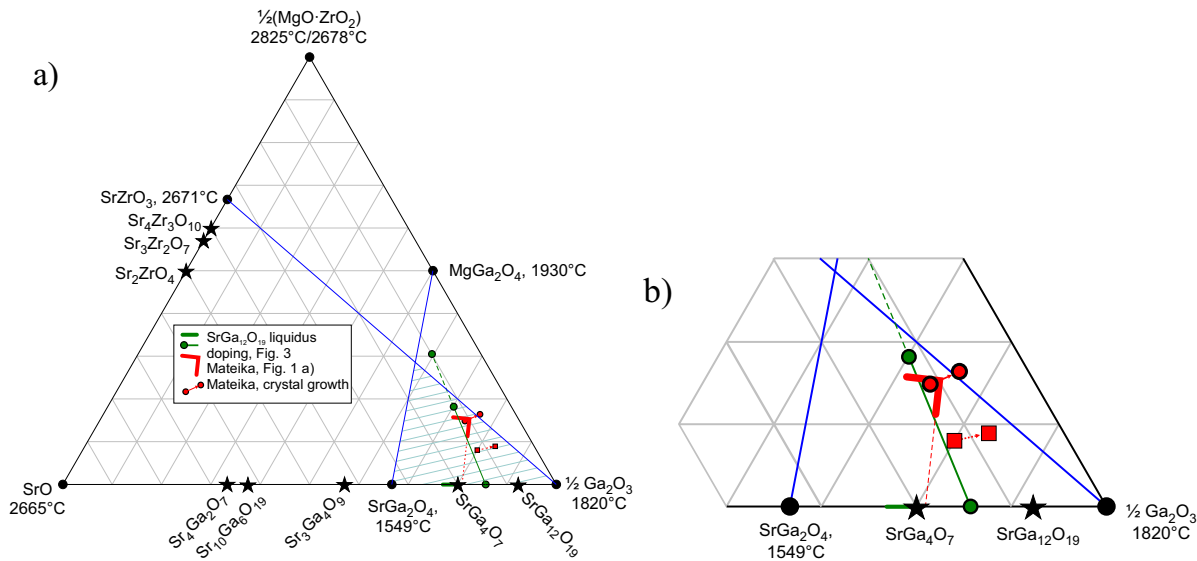


Figure 4: a) Concentration triangle $\text{SrO}-\frac{1}{2}\text{Ga}_2\text{O}_3-\frac{1}{2}(\text{MgO}-\text{ZrO}_2)$. Compounds with congruent melting points are marked by circles ●, with peritectic melting by asterisks ★. Blue tie lines $\text{SrZrO}_3-\text{Ga}_2\text{O}_3$ and $\text{MgGa}_2\text{O}_4-\text{SrGa}_2\text{O}_4$ separate independent partial systems. Data of Mateika & Laurien [15] and from this study added. b) Ga_2O_3 rich corner of the triangle.

- [9] L. M. Kovba, L. N. Lykova, V. P. Kobzareva, L. M. Lopato, A. V. Shevchenko, Phase diagram of the system $\text{BaO}-\text{Ga}_2\text{O}_3$, *Neorganičeskie Materialy* 20 (1975) 1970–1973.
- [10] Z. R. Kadyrova, N. A. Sirazhiddinov, S. K. Tuganova, Investigation of the systems $\text{SrAl}_{12}\text{O}_{19}-\text{Ca}(\text{Ba})\text{Al}_{12}\text{O}_{19}$ and $\text{SrGa}_{12}\text{O}_{19}-\text{BaGa}_{12}\text{O}_{19}$, *Neorg. Mater.* 33 (1997) 360–363.
- [11] N. Solak, Interface stability in solid oxide fuel cells for intermediate temperature applications, Ph.D. thesis, Universität Stuttgart (2007). doi:10.18419/opus-872.
- [12] A. N. Richter, Stabilität, Kristallchemie, Strukturen und optische Eigenschaften von Hexaphasen in $\text{CaO}/\text{SrO}/\text{BaO}-\text{Al}_2\text{O}_3/\text{Ga}_2\text{O}_3-\text{MgO}/\text{MnO}_x$ Systemen, Ph.D. thesis, Friedrich-Alexander-Universität, Erlangen-Nürnberg (2012).
- [13] F. Haberey, R. Leckebusch, K. Sahl, M. Rosenberg, Zur Züchtung von $\text{SrGa}_{12}\text{O}_{19}$ -Einkristallen, *Naturwissenschaften* 66 (1979) 617.
- [14] F. Haberey, R. Leckebusch, M. Rosenberg, K. Sahl, Flux growth of $\text{SrGa}_{12}\text{O}_{19}$ crystals, *J. Crystal Growth* 61 (1983) 284–288. doi:10.1016/0022-0248(83)90364-0.
- [15] D. Mateika, R. Laurien, Czochralski growth of solid solutions of strontium hexagallate with magnesium and zirconium as dopants, *J. Crystal Growth* 52 (1981) 566–572. doi:10.1016/0022-0248(81)90341-9.
- [16] D. Mateika, C. Rusche, Coupled substitution of gallium by magnesium and zirconium in single crystals of gadolinium gallium garnet, *J. Crystal Growth* 42 (1977) 440–444. doi:10.1016/0022-0248(77)90229-9.
- [17] R. Ropp, Encyclopedia of the Alkaline Earth Compounds, Elsevier, Amsterdam, 2013, Ch. Group 13 (B, Al, Ga, In and Tl) Alkaline Earth Compounds, pp. 481–635. doi:10.1016/B978-0-444-59550-8.00006-5.
- [18] www.factsage.com, FactSage 7.3, GTT Technologies, Kaiserstr. 100, 52134 Herzogenrath, Germany (2019).
- [19] V. Kahlenberg, The crystal structures of the strontium gallates $\text{Sr}_{10}\text{Ga}_6\text{O}_{19}$ and $\text{Sr}_3\text{Ga}_2\text{O}_6$, *J. Solid State Chemistry* 160 (2001) 421–429. doi:10.1006/jssc.2001.9259.
- [20] H. Krüger, B. Lazić, E. Arroyabe, V. Kahlenberg, Modulated structure and phase transitions of $\text{Sr}_{10}\text{Ga}_6\text{O}_{19}$, *Acta Cryst. B: Structural Science* 65 (2009) 587–592. doi:10.1107/S0108768109026974.
- [21] R. C. Pullar, Hexagonal ferrites: A review of the synthesis, properties and applications of hexaferrite ceramics, *Prog. Mat. Sci.* 57 (7) (2012) 1191–1334. doi:10.1016/j.pmatsci.2012.04.001.
- [22] H. Graetsch, W. Gebert, Positional and thermal disorder in the trigonal bipyramid of magnetoplumbite structure type $\text{SrGa}_{12}\text{O}_{19}$, *Z. Krist. – Crystalline Materials* 209 (4) (1994) 338–342. doi:10.1524/zkri.1994.209.4.338.
- [23] R. D. Shannon, Revised effective ionic radii and systematic studies of interatomic distances in halides and chalcogenides, *Acta Cryst. A* 32 (1976) 751–767. doi:10.1107/S0567739476001551.
- [24] W. J. M. van der Kemp, J. G. Blok, P. R. van der Linde, H. A. J. Oonk, A. Schuijff, M. L. Verdonk, Binary alkaline earth oxide mixtures: Estimation of the excess thermodynamic properties and calculation of the phase diagrams, *Calphad* 18 (1994) 255–267. doi:https://doi.org/10.1016/0364-5916(94)90032-9.
- [25] S. Singh, V. Jancik, H. W. Roesky, R. Herbst-Irmer, Synthesis, characterization, and X-ray crystal structure of a gallium monohydroxide and a hetero-bimetallic gallium zirconium oxide, *Inorganic Chemistry* 45 (2006) 949–951. doi:10.1021/ic0517691.
- [26] S. M. Lakiza, L. M. Lopato, Stable and metastable phase relations in the system aluminazirconiatrytria, *J. Amer. Ceram. Soc.* 80 (1997) 893–902. doi:10.1111/j.1151-2916.1997.tb02919.x.
- [27] ACerS and NIST, Phase Equilibria Diagrams, V. 4.0, entry Zr-082 (2013).
- [28] M. Zinkevich, S. Geupel, F. Aldinger, Thermodynamic assessment of the ternary systems $\text{Ga}-\text{Mg}-\text{O}$, $\text{Ga}-\text{Ni}-\text{O}$, $\text{Mg}-\text{Ni}-\text{O}$ and extrapolation to the $\text{Ga}-\text{Mg}-\text{Ni}-\text{O}$ phase diagram, *J. Alloys Compd.* 393 (2005) 154–166. doi:10.1016/j.jallcom.2004.09.069.
- [29] Z. Galazka, D. Klimm, K. Irmischer, R. Uecker, M. Pietsch, R. Bertram, M. Naumann, M. Albrecht, A. Kwasniewski, R. Schewski, M. Bickermann, MgGa_2O_4 as a new wide bandgap transparent semiconducting oxide: growth and properties of bulk single crystals, *phys. stat. sol. (a)* 212 (2015) 1455–1460. doi:10.1002/pssa.201431835.
- [30] P. Paufler, Phasendiagramme, Akademie-Verlag, Berlin, 1981.
- [31] P. J. Majewski, M. Rozumek, H. Schluckwerder, F. Aldinger, Phase diagram studies in the systems $\text{La}_2\text{O}_3-\text{SrO}-\text{Ga}_2\text{O}_3$, $\text{La}_2\text{O}_3-\text{MgO}-\text{La}_2\text{O}_3$, and $\text{SrO}-\text{MgO}-\text{Ga}_2\text{O}_3$ at 1400 °C in air, *J. Amer. Ceram. Soc.* 84 (2001) 1093–1096. doi:10.1111/jace.2001.84.issue-5.